

**8th Baltic Electrochemistry Conference:
Finding New Inspiration 2**



Dual-transition metal and nitrogen co-doped silicon oxycarbide-based catalysts for oxygen reduction at the high temperature PEM fuel cell cathode

Marek Mooste, Dana Schonvogel, Michaela Wilhelm, Peter Wagner, Kaspar Andreas Friedrich

Dr. Marek Mooste (Postdoctoral Researcher)

15.04.2024



Introduction



- The modern lifestyle and progressive economic growth - ever-increasing, global energy consumption, speeding up the climate change.
- The global dependency on fossil fuel has disadvantages (carbon and pollutant emissions), CO₂, NO_x, SO_x, particulate matter.
- Research on clean, efficient, and more sustainable energy technologies. **Fuel cells** have been recognized as possible energy conversion devices for mobile and stationary applications.

DLR (German Aerospace Center)

- More than 9000 employees work in 54 institutes and facilities
- 30 sites across Germany
- DLR Institute of Engineering Thermodynamics - Location Oldenburg

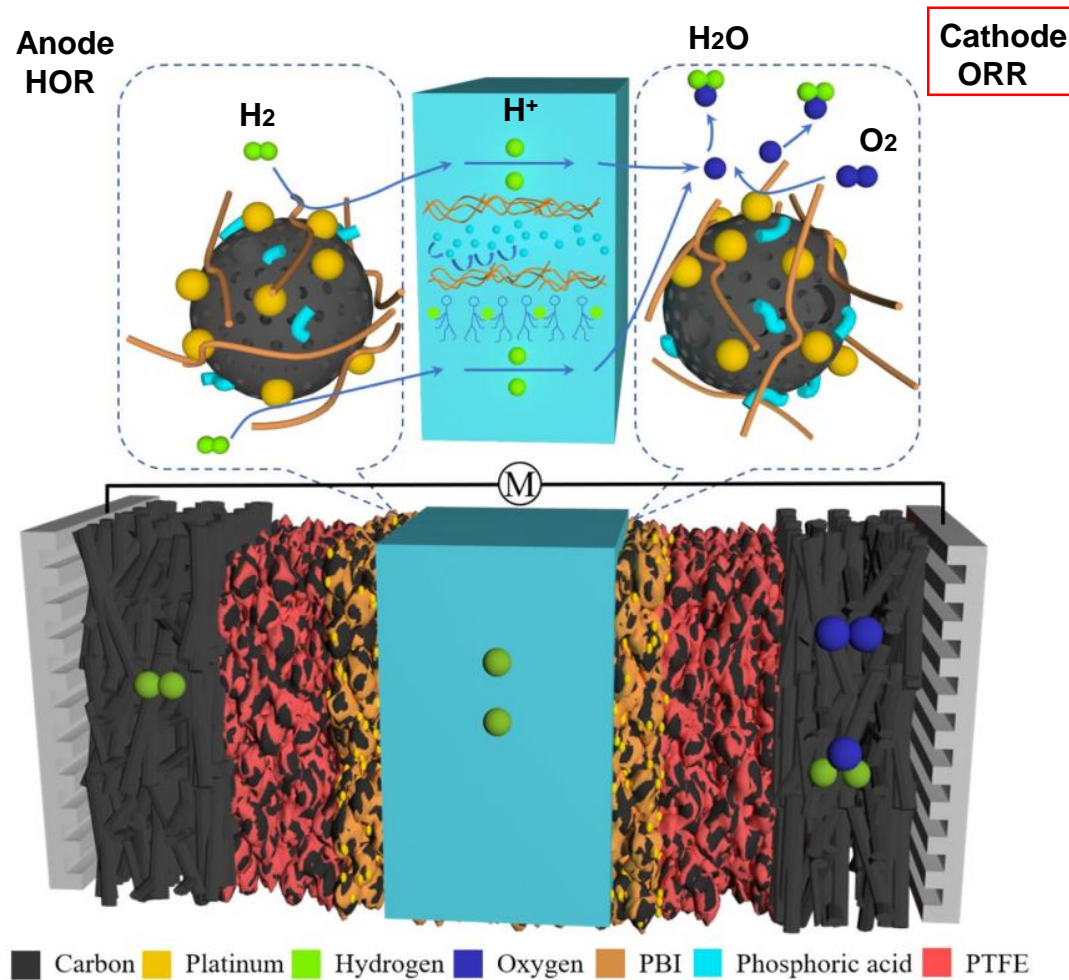
High-temperature polymer electrolyte membrane fuel cell (HT-PEM) workgroup

[DOI: 10.1039/d3ta06895a](https://doi.org/10.1039/d3ta06895a)

[DOI: 10.1002/adma.202302207](https://doi.org/10.1002/adma.202302207)



High temperature PEM fuel cell (HT-PEMFC)

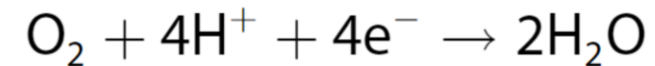


HT-PEMFC is environmentally friendly energy conversion device suitable for heavy-duty transport, stationary, and aviation applications.

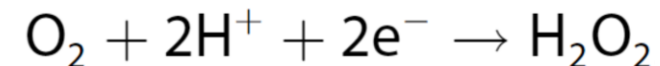
Hot HT-PEMFC topic: the development of efficient Pt-group-metal (PGM)-free **oxygen reduction reaction (ORR)** catalyst for the fuel cell cathode.

ORR pathways:

4 electrons (e.g. Pt/C)



2 electrons (peroxide production)



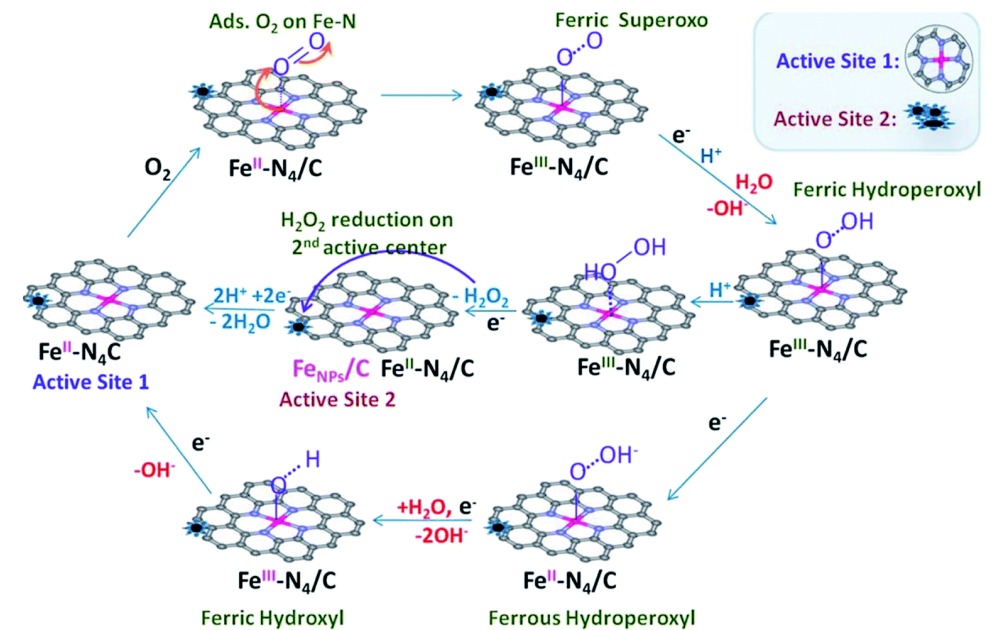
Scheme 1. Schematic representation of the structure of HT-PEMFCs. The relative sizes and distances are not to scale, and the catalyst layer, binder, filler, MPL, and carbon fibers possess significantly different porosities and sizes. [DOI: 10.1007/s41918-023-00180-y](https://doi.org/10.1007/s41918-023-00180-y)

M-N-C cathode catalyst materials

- Most promising materials have been developed based on the transition metal and nitrogen co-doped nanocarbon materials (M-N-C).
- Nanocarbon materials:** graphene, multi-walled carbon nanotubes (MWCNT), carbide-derived carbons (CDC), polymer-derived carbon (PDC) etc.
 - high surface area, high durability, good electrical conductivity

Transition metal (TM) and nitrogen co-doping:

- transition metal (e.g. Fe, Co, Mn) ion coordinated to nitrogen sites (**Me-N_x**)
- active N species
- transition metal nanoparticles
 - provide active sites for ORR



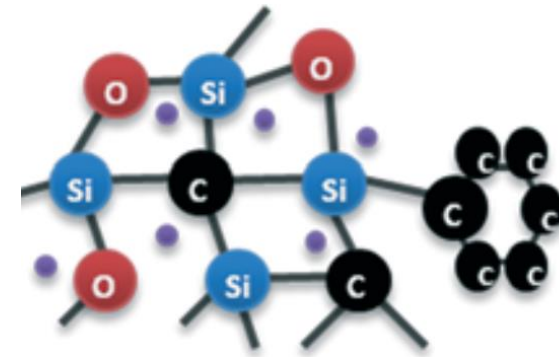
[DOI: 10.1021/jp500781v](https://doi.org/10.1021/jp500781v)

Dual metal M-N-C catalysts

The main aim:

Preparation of **dual metal** M-N-C materials for HT-PEMFC cathode (M-N-C type)

1. Catalyst support/carbon backbone:
Silicon oxycarbide (SiOC) based materials
2. Dual atom metal combinations (supported by literature):
 1. Fe/Co
 2. Fe/Mn
 3. Fe/Cu



Previous collaborations with University of Bremen.

SiOC-based M-N-C were found to be suitable for Fuel cell cathode catalyst application.

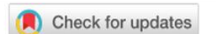
Issue 3, 2019



From the journal:
Catalysis Science & Technology

[Previous Article](#) | [Next Article](#)

Polymer-derived Co/Ni-SiOC(N) ceramic electrocatalysts for oxygen reduction reaction in fuel cells†



Thamires Canuto de Almeida e Silva, ^a Marek Mooste, ^b Elo Kibena-Pöldsepp, ^b Leonard Matisen, ^c Mairo Merisalu, ^{bc} Mati Kook, ^c Väino Sammelselg, ^{bc} Kaido Tammeveski, ^{ab} Michaela Wilhelm ^{ad} and Kuroschi Rezwan ^{ad}

[DOI: 10.1039/c8cy02207k](https://doi.org/10.1039/c8cy02207k)

Catalyst preparation

1. Polymer-derived carbon (PDC) precursor materials (**University of Bremen**):

1. Powders of *poly(methyl phenyl silsesquioxane)*, *poly(methylsilsesquioxane)*, *graphite*, *azodicarboxamide*, and *(3-Aminopropyl)triethoxysilane*, *imidazole*, *metal acetylacetonates* dispersed in xylene.
2. Pyrolysed, ball-milled, sieved → PDC precursor materials:
PDC, MnFe-PDC, CoFe-PDC, CuFe-PDC

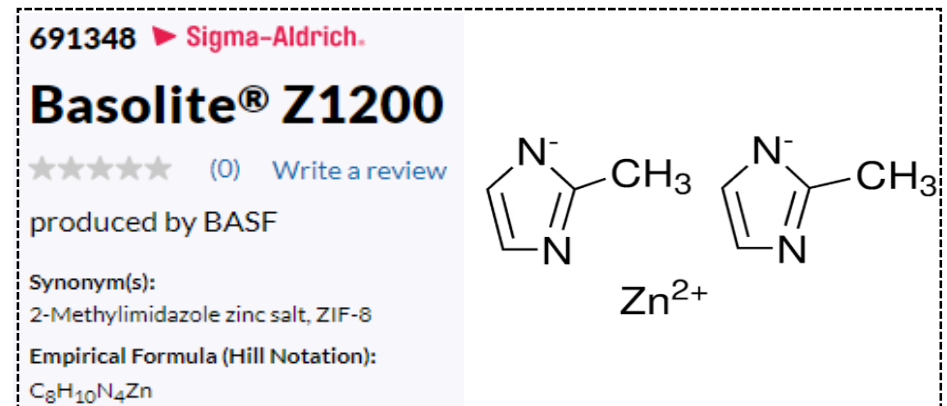
2. Functionalisation with N-source ZIF-8 (Basolite® Z1200) (**DLR**):

1. Mixed 50/50 wt% of PDC/ZIF-8 in methanol, drying.
2. Pyrolysed at 950 °C → N-SiOC catalyst materials:
MnFe-N-SiOC, CoFe-N-SiOC, CuFe-N-SiOC

*3. *Acid leaching:*

2M sulfuric acid for 16 h at 90 °C followed by second pyrolysis:

MnFe-SiOC-Acid, CoFe-SiOC-Acid, CuFe-SiOC-Acid



Physical characterisation of ZIF-8 modified PDC materials

Scanning electron microscopy (SEM)

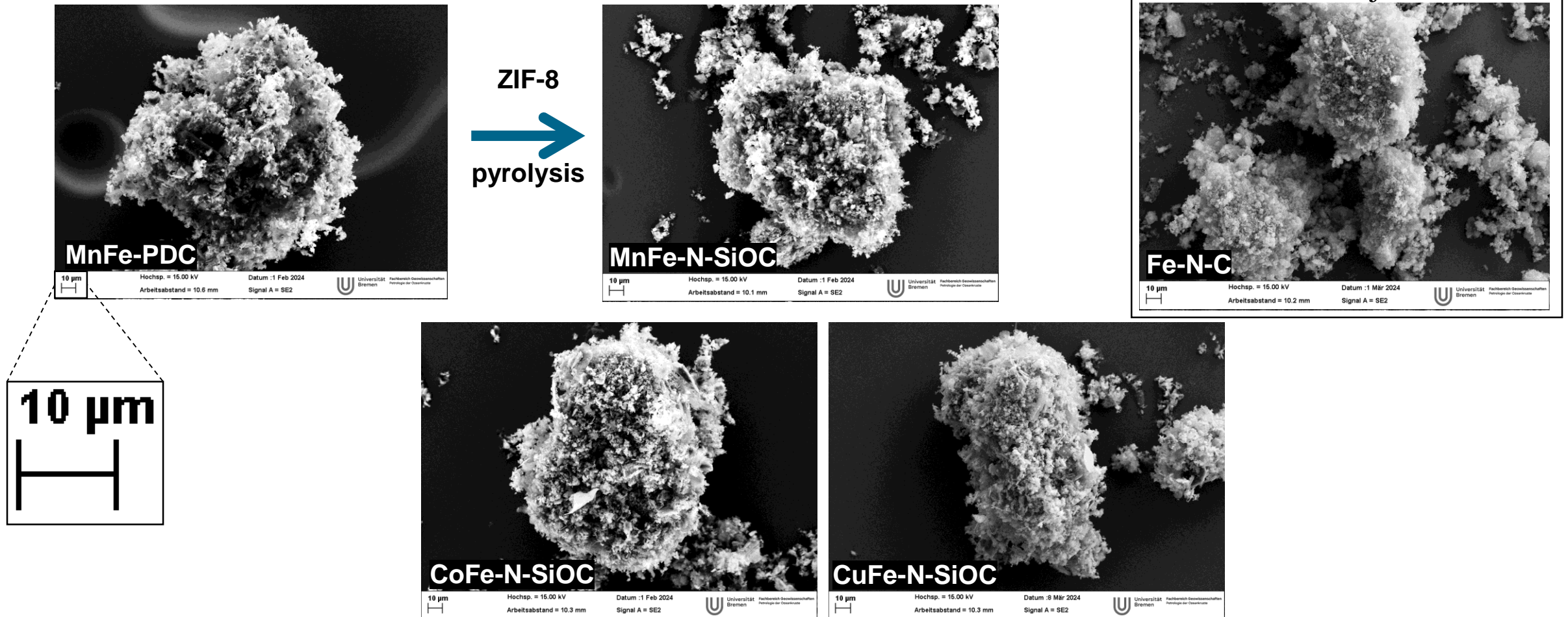


Fig. 1. SEM images of different materials. The FeMn-based material is shown before (-PDC) and after modification with ZIF-8 via pyrolysis at 950 °C (-N-SiOC). The commercial Fe-N-C is also shown for comparison.

Physical characterisation of ZIF-8 modified PDC materials



Energy-dispersive X-ray spectroscopy (EDS)

	PDC	CoFe-PDC	CoFe-N-SiOC	MnFe-PDC	MnFe-N-SiOC	CuFe-PDC	CuFe-N-SiOC
C	73.7 ± 1.9	77.1 ± 3.5	75.5 ± 0.9	76.9 ± 1.0	78.4 ± 1.5	74.6 ± 7.4	76.8 ± 2.4
N	2.70 ± 0.13	3.38 ± 0.13	6.30 ± 0.42	3.61 ± 0.28	6.71 ± 1.03	2.77 ± 1.26	7.34 ± 0.71
O	18.3 ± 1.5	15.1 ± 2.4	13.3 ± 1.3	13.2 ± 0.7	10.3 ± 0.8	16.5 ± 4.8	12.1 ± 1.2
Si	5.36 ± 0.67	4.04 ± 0.77	4.14 ± 0.62	5.65 ± 0.89	3.85 ± 0.35	4.78 ± 1.19	2.81 ± 1.49
Fe	-	0.21 ± 0.08	0.23 ± 0.05	0.35 ± 0.07	0.26 ± 0.04	0.25 ± 0.06	0.21 ± 0.06
Mn	-	-	-	0.29 ± 0.06	0.20 ± 0.06	-	-
Co	-	0.20 ± 0.06	0.20 ± 0.07	-	-	-	-
Cu	-	-	-	-	-	0.26 ± 0.12	0.38 ± 0.13
Zn	-	-	0.29 ± 0.10	-	0.28 ± 0.15	-	0.28 ± 0.14

Table 1. Elemental composition (at%) of different materials. After the modification of precursor material (-PDC) with ZIF-8 via pyrolysis at 950 °C (-N-SiOC), the introduction of **Zn and increase in **N** amount is observed.**

Physical characterisation of ZIF-8 modified PDC materials

High-resolution transmission electron microscopy (HR-TEM)

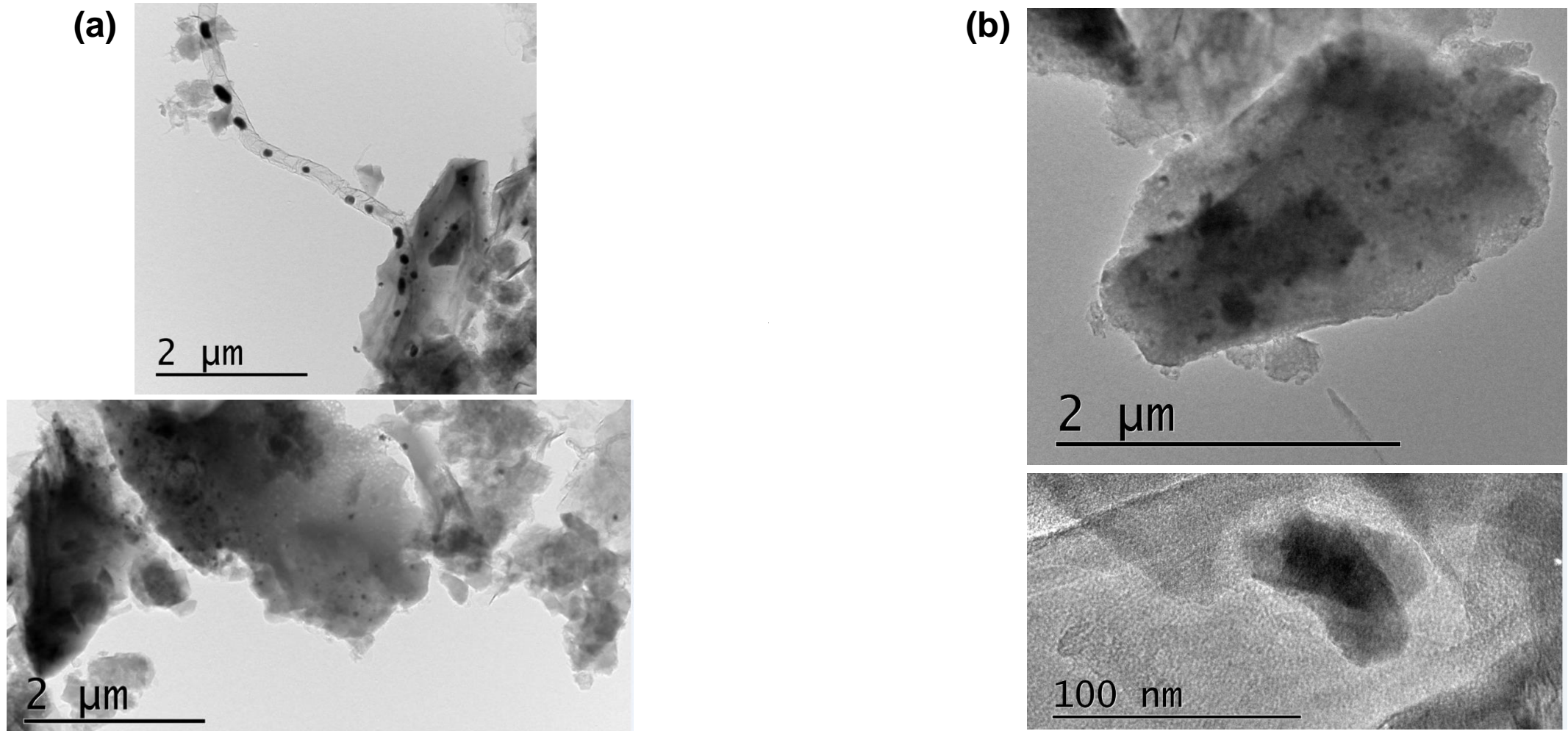


Fig. 2. HR-TEM images of different materials after ZIF-8 modification, (a) CuFe-N-SiOC, (b) MnFe-N-SiOC.

Physical characterisation of ZIF-8 modified PDC materials

X-ray photoelectron spectroscopy (XPS)

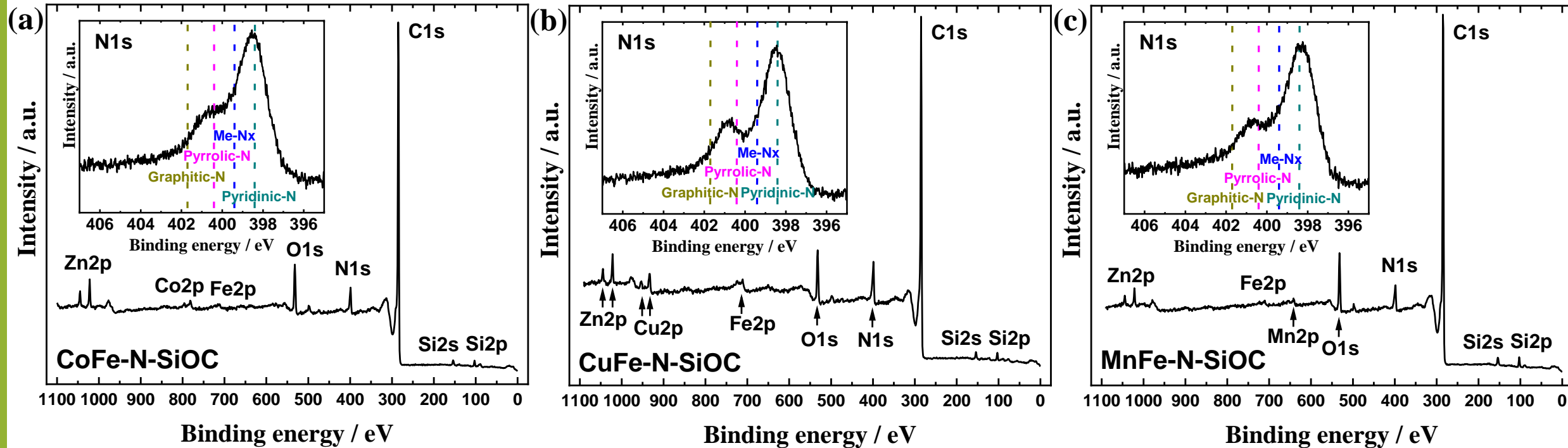


Fig. 3. XPS survey spectra of different catalyst materials after the modification with ZIF-8 via pyrolysis at 950 °C (-N-SiOC). The insets show the high-resolution spectrum in the N1s region for the corresponding material.

RRDE half-cell testing (Rotating ring-disk electrode)

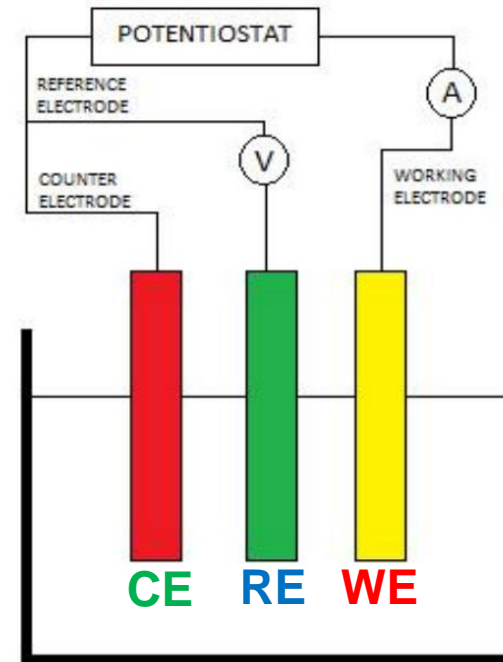


LSV recorded at 1600 rpm



WE1: ORR current
WE2: Peroxide oxidation current

From WE1/WE2 difference – peroxide yield and electron transfer number per O₂ molecule



DOI: [10.1088/1757-899X/340/1/012017](https://doi.org/10.1088/1757-899X/340/1/012017)

WE1: M-N-C catalyst on GC
WE2: Pt ring
RE: MMS (converted to RHE)
CE: Pt wire
Electrolyte: 0.5 M H₃PO₄, 23 °C



https://www.metrohm.com/en/products/a/ut_r/aut_rrde_s.html

RRDE half-cell testing for ORR in 0.5 M H₃PO₄ at 23 °C

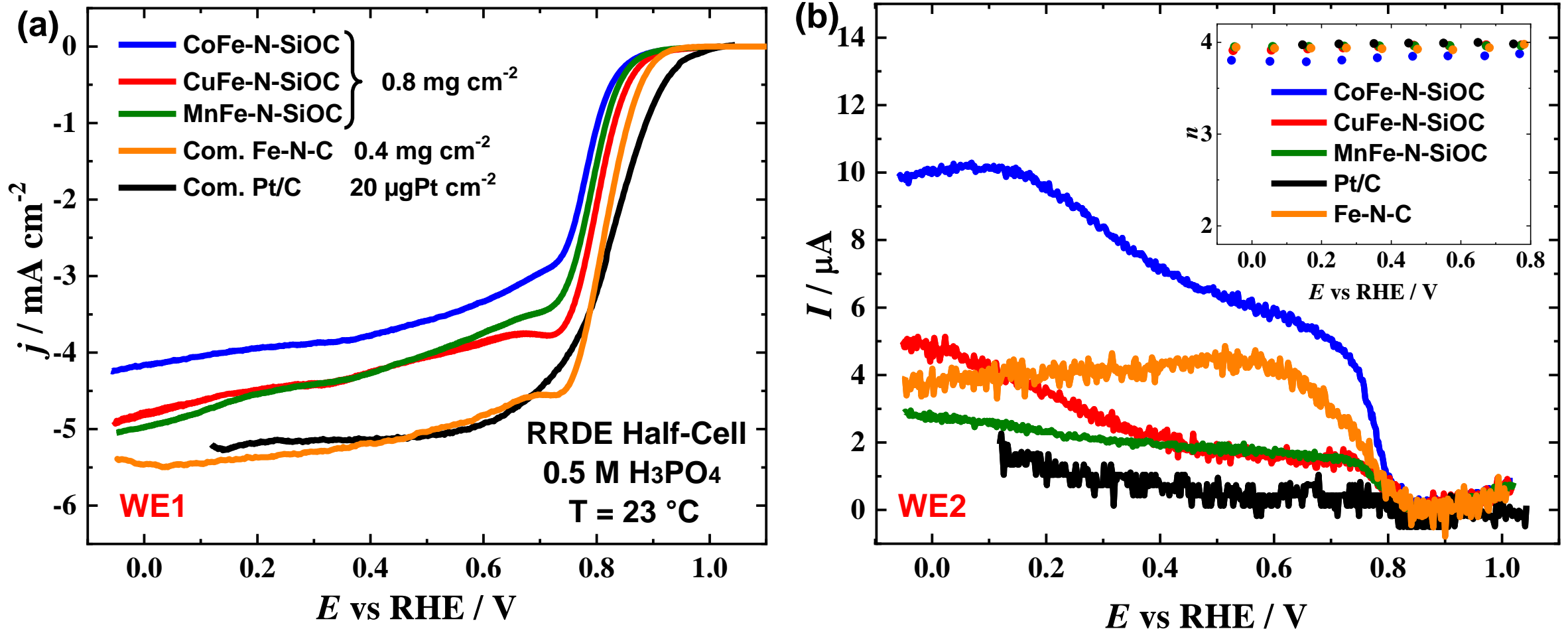


Fig. 4. (a) Disc current density, (b) ring current and electron transfer numbers (n) for different catalyst coated GC-disk/Pt-ring electrodes recorded at 1600 rpm in O₂-saturated phosphoric acid solution.

RRDE half-cell testing for ORR in 0.5 M H₃PO₄ at 23 °C

Catalyst	$E_{1/2}$	MA _{0.75V}	MA _{0.80V}
CoFe-N-SiOC	770 ± 3	3.41 ± 0.14	1.25 ± 0.10
MnFe-N-SiOC	774 ± 2	3.63 ± 0.08	1.80 ± 0.07
CuFe-N-SiOC	781 ± 6	3.67 ± 0.37	2.20 ± 0.14
Fe-N-C	808 ± 2	11.03 ± 0.14	7.56 ± 0.15
Pt/C (20wt. Pt)	824 ± 3	29.73 ± 2.33	37.35 ± 2.91

Table 2. Half-wave potential ($E_{1/2}$, unit mV vs. RHE) and mass activity (MA, unit A g_{Catalyst}⁻¹) values at 0.75 V and 0.80 V for ORR derived from the disc currents of RRDE measurements performed at 1600 rpm.

Acid leaching (2 M H₂SO₄) influence on RRDE results

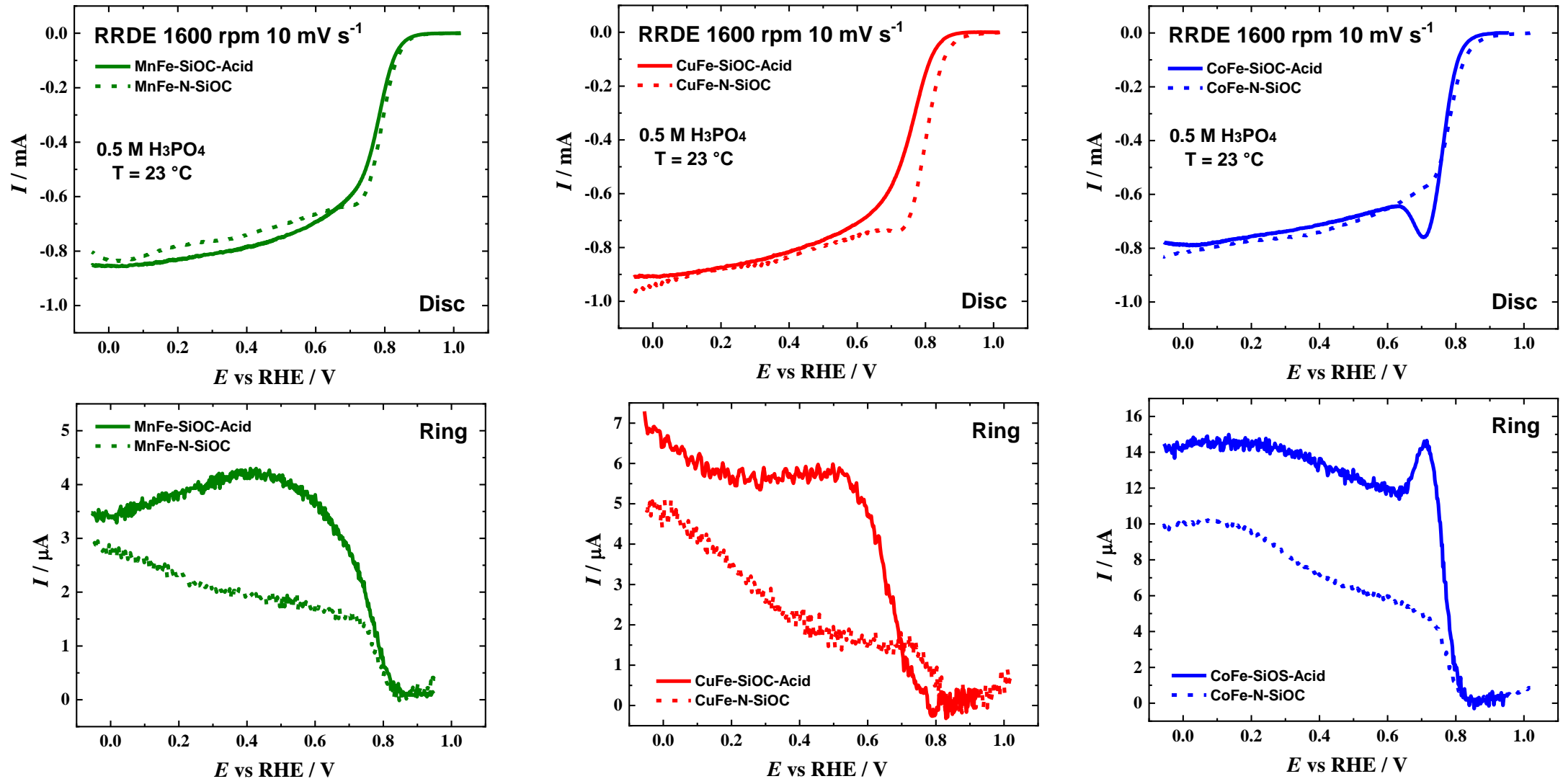


Fig. 5. Acid leaching route is in 2 M sulfuric acid for 16 h at 90 °C + second pyrolysis (*Not beneficial for peroxide yield*)

Acid leaching (2 M H₂SO₄) influence on RRDE results

Catalyst	$E_{1/2}$	MA _{0.75V}	MA _{0.80V}
CoFe-SiOC	770 ± 3	3.41 ± 0.14	1.25 ± 0.10
CoFe-SiOC-Acid	772 ± 2	↑ 3.74 ± 0.18	23% ↓ 0.96 ± 0.09
MnFe-SiOC	774 ± 2	3.63 ± 0.08	1.80 ± 0.07
MnFe-SiOC-Acid	↓ 757 ± 6	↓ 2.99 ± 0.17	30% ↓ 1.26 ± 0.11
CuFe-SiOC	781 ± 6	3.67 ± 0.37	2.20 ± 0.14
CuFe-SiOC-Acid	↓ 726 ± 8	↓ 2.26 ± 0.23	58% ↓ 0.91 ± 0.09

Table 3. Half-wave potential ($E_{1/2}$, unit mV vs. RHE) and mass activity (MA, unit A g_{Catalyst}⁻¹) values at 0.75 V and 0.80 V for ORR derived from the disc currents of RRDE measurements performed at 1600 rpm.

RDE half-cell stability testing for ORR in 0.5 M H₃PO₄ at 23 °C

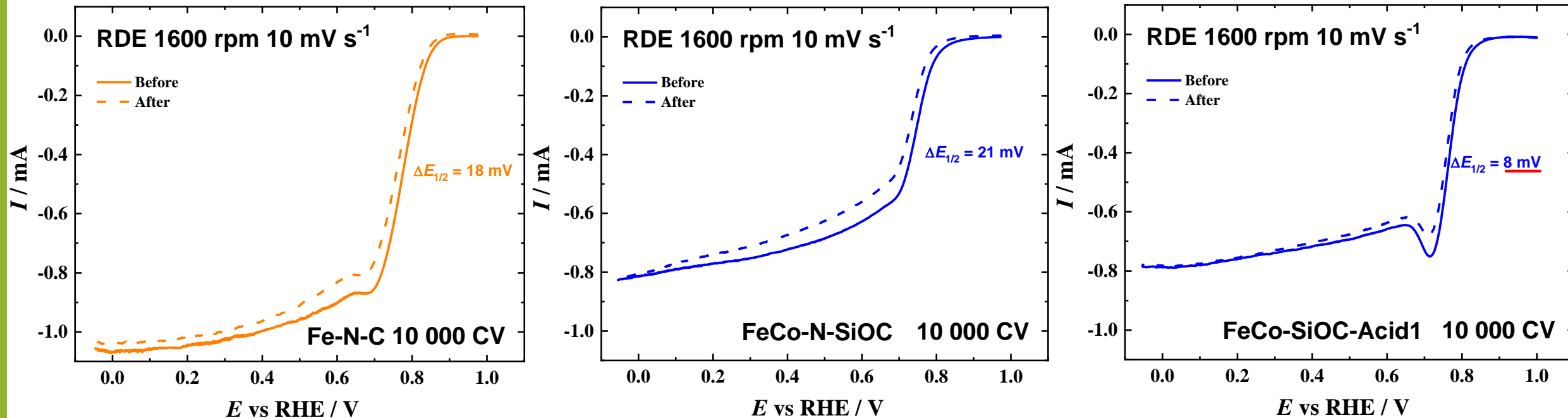


Fig. 6. RDE voltammetry curves recorded at 1600 rpm before and after stability testing for 10 000 cyclic voltammetry (CV) cycles in O₂- saturated 0.5 M H₃PO₄ solution. Commercial Fe-N-C (PMF-0011904, Pajarito Powder) is included for comparison.

(26 h CV test in 400 mV potential window)

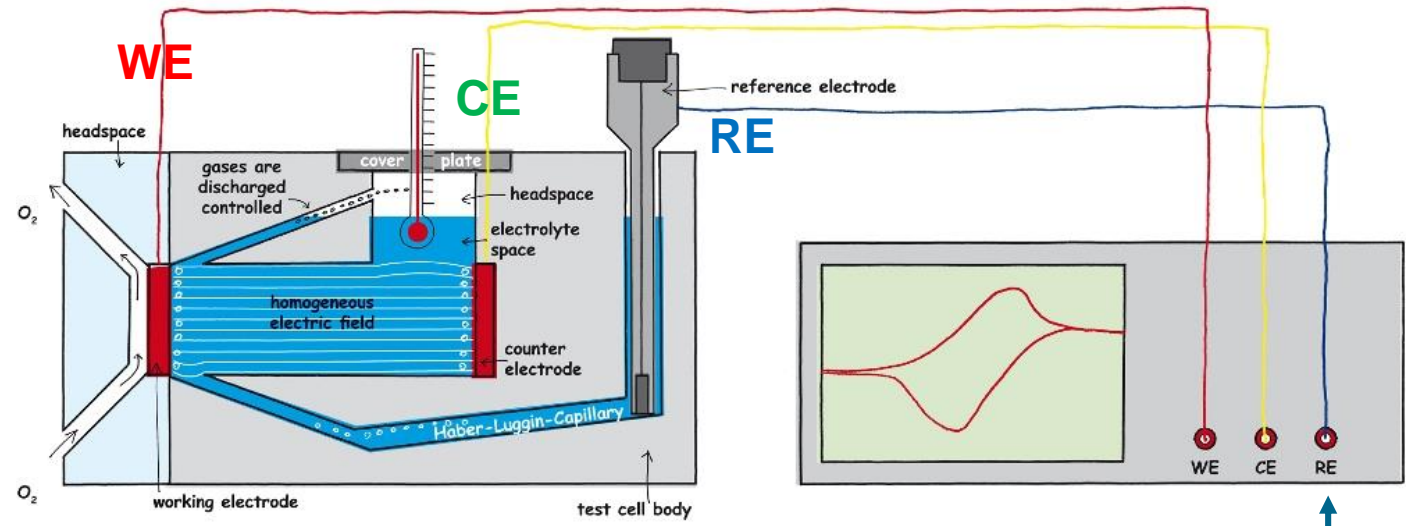
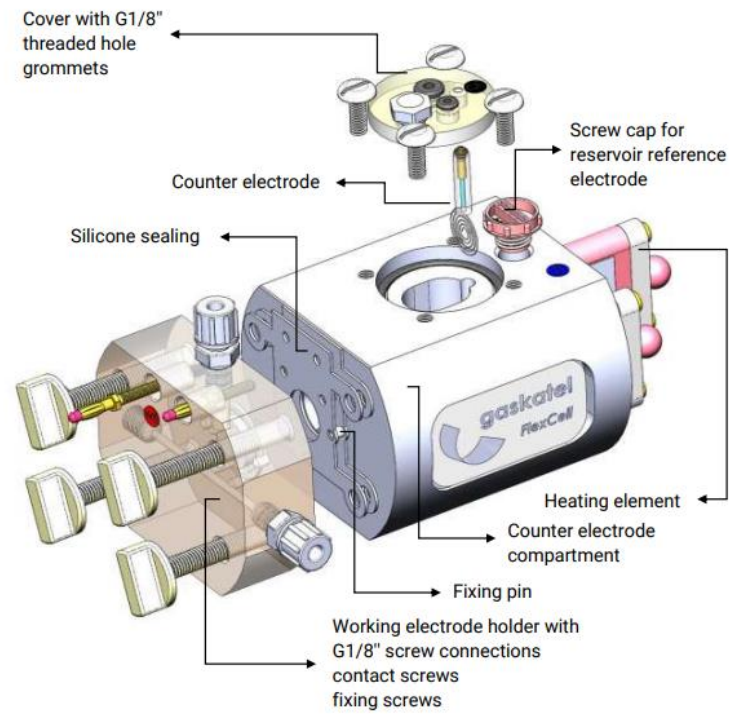
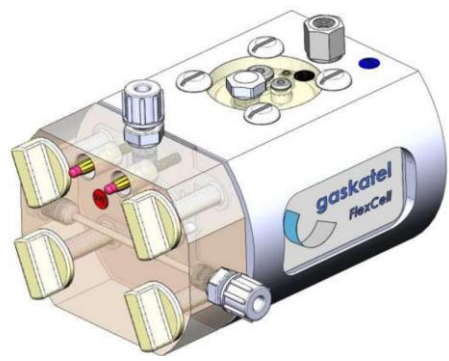
GDE half-cell testing

(Gas diffusion electrode)



Test Cell FlexCell

Voltammetric Test Cell PTFE / PP



- WE:** M-N-C catalyst, 3 mg cm⁻² (coated on commercial GDL)
- RE:** RHE
- CE:** Pt wire
- Electrolyte:** conc. H₃PO₄, 160 °C (+ PBI membrane between M-N-C and electrolyte)



<https://gaskatel.de/en/test-cells-for-the-electrochemistry/>

GDE half-cell testing for ORR (conc. H_3PO_4 at $160\text{ }^\circ\text{C}$)

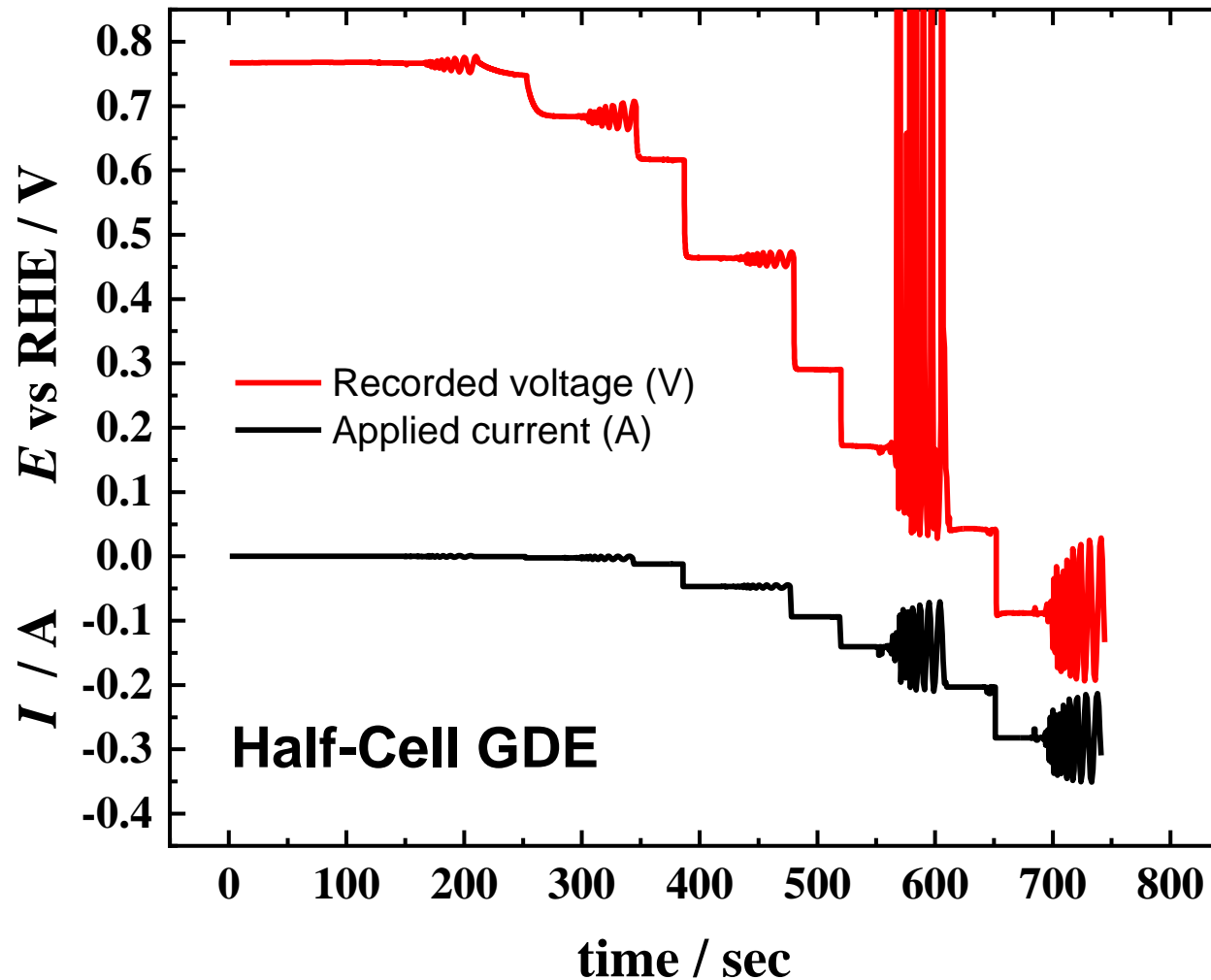


Fig. 7. Measurement consists of chronopotentiometry followed by impedance spectroscopy at certain current value steps (e.g. -0.3 mA , -2.35 mA , -11.8 mA -280 mA). Resistance value is used for iR -drop compensation at certain current.

GDE half-cell testing for ORR (conc. H_3PO_4 at $160\text{ }^\circ\text{C}$)

(Single measurement with each catalyst material)

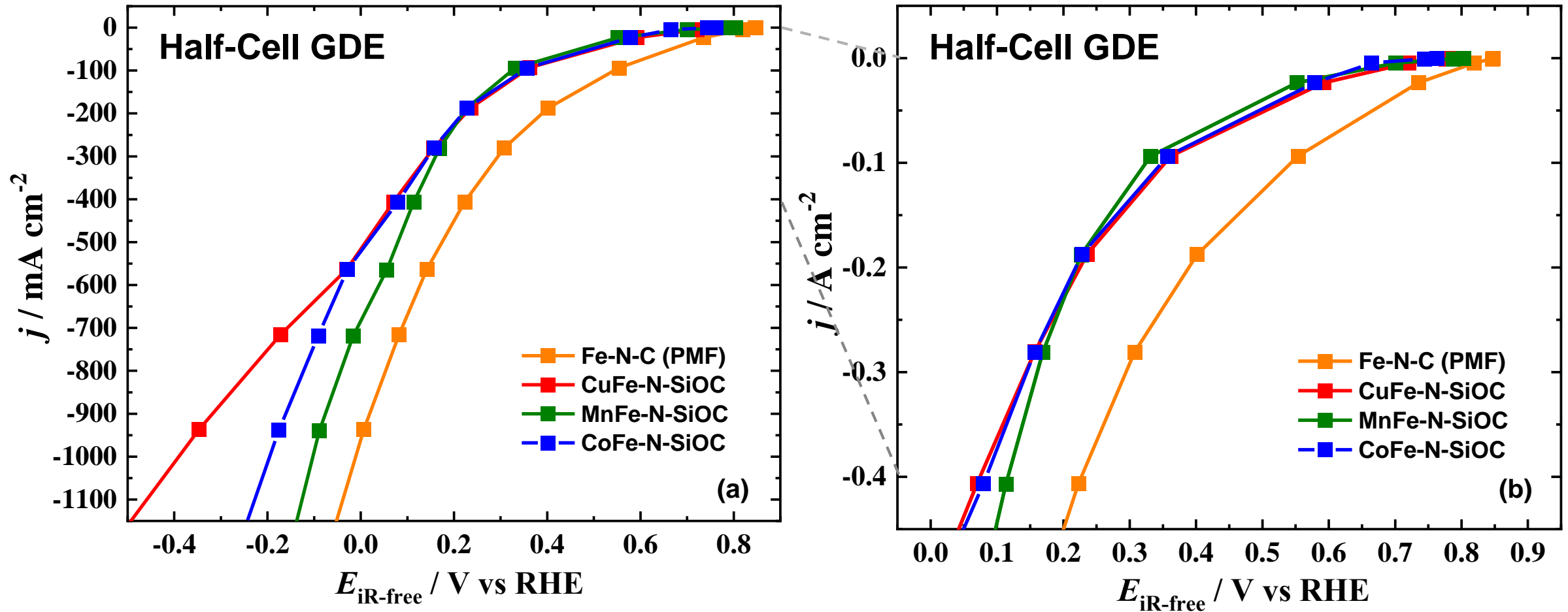


Fig. 8. GDE half-cell polarisation curves. Shown data points have been obtained via chronopotentiometry measurements corrected for iR -drop value using the impedance spectroscopy at corresponding current value.

GDE testing (acid leaching influence)

(Averaged measurement results with each catalyst material)

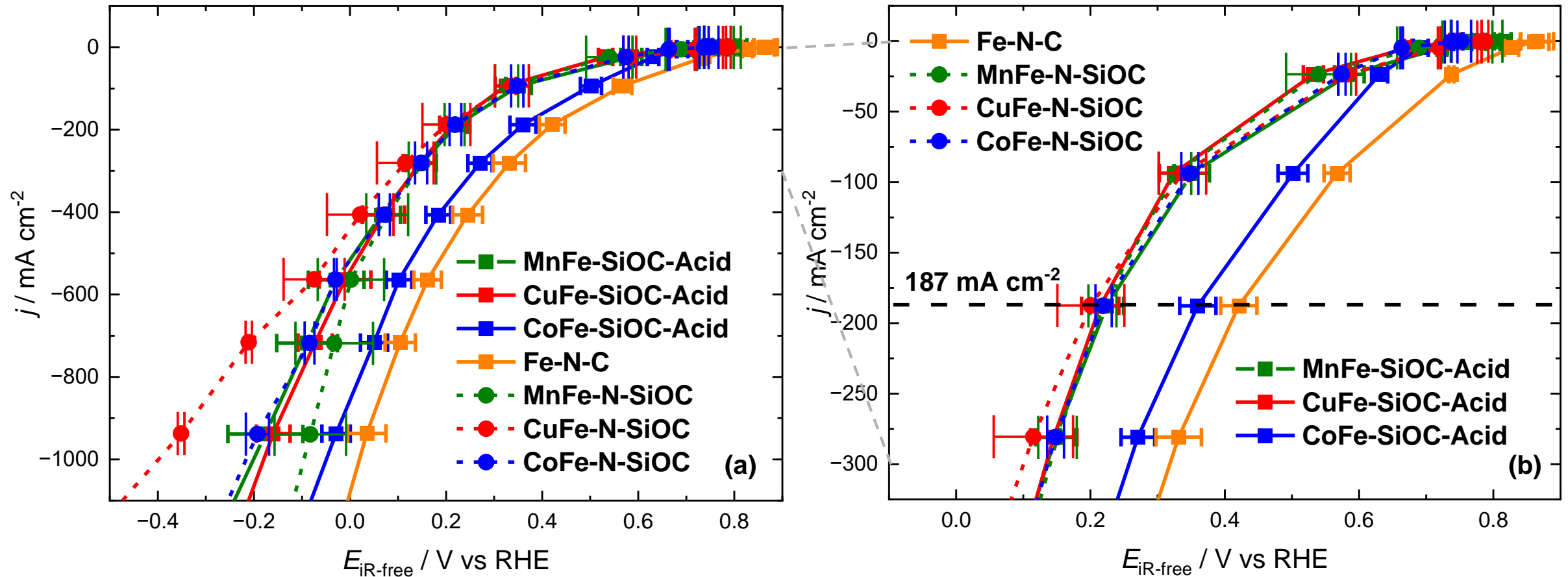


Fig. 9. GDE half-cell polarisation curves. Acid leaching route is in 2 M sulfuric acid for 16 h at 90 °C + second pyrolysis.

GDE testing (acid leaching influence)

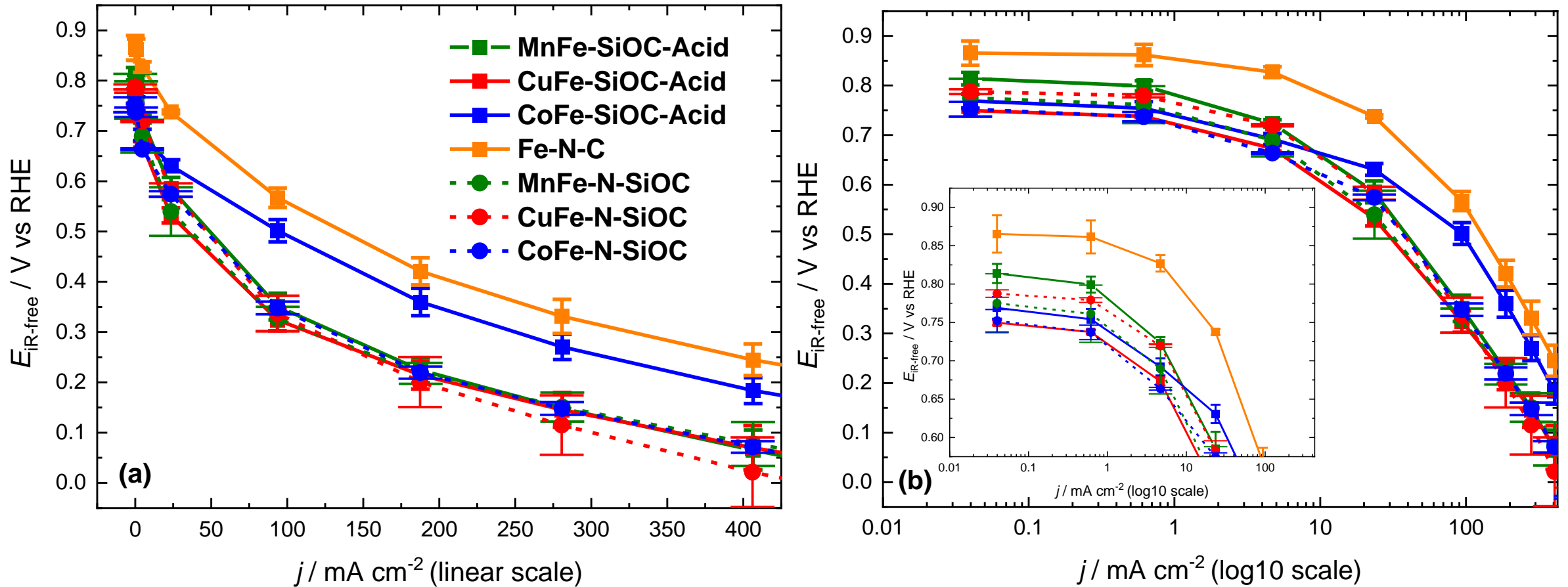


Fig. 10. Investigation of low current density region (ca. 0.9 - 0.6 V) using the logarithmic scale for current density.

GDE testing and acid leaching influence



Catalyst	OCP	E_{187}
CoFe-N-SiOC	752 ± 15	219 ± 12
<u>CoFe-SiOC-Acid</u>	17 mV ↑ 769 ± 14	64% ↑ 360 ± 27
MnFe-N-SiOC	775 ± 38	218 ± 21
MnFe-SiOC-Acid	39 mV ↑ 814 ± 12	~3% ↑ 224 ± 25
CuFe-N-SiOC	788 ± 15	201 ± 50
CuFe-SiOC-Acid	38 mV ↓ 750 ± 13	~6% ↑ 214 ± 28
Fe-N-C	865 ± 24	421 ± 27

Table 4. Open circuit potential (OCP, unit mV vs. RHE) and potential value at 187 mA cm⁻² (E_{187} , unit mV vs. RHE) for ORR derived from the GDE polarisation curves with different cathode catalyst materials.

Conclusions



Dual transition metal containing SiOC materials

Functionalised with N using ZIF-8 and pyrolysis method

RRDE half-cell testing for ORR in 0.5 M H₃PO₄, 23 °C:

- CuFe and MnFe-containing materials more promising at RT ($E_{1/2}$, n value)
- CoFe material showed an increase in ORR activity and long-term stability after acid treatment
- Acid treatment not beneficial for CuFe and MnFe-containing materials

GDE half-cell testing for ORR with conc. H₃PO₄ at 160 °C:

- Acid treated and non-treated CuFe and MnFe-containing materials similar
 - *MnFe material showed considerable increase in OCP value after acid treatment*
- CoFe material showed a considerable increase in ORR activity after acid treatment

(Manuscript under preparation)

Aknowledgements



Advanced Ceramics group at the University of Bremen:

Dr. Michaela Wilhelm



DLR Institute of Engineering Thermodynamics:

Dr. Dana Schonvogel

Mr. Peter Wagner

Prof. Dr. Kaspar Andreas Friedrich

Colleagues at DLR for technical support and supervision



Deutscher Akademischer Austauschdienst
German Academic Exchange Service

Funding:

DLR, German Academic Exchange Service (DAAD), Estonian Research Council (ETAG)

DLR-DAAD Research Fellowship (11.2022 – 10.2023)
PUTJD1170 Postdoctoral research grant (11.2023 – ...)



Thank you for your kind attention!

Questions?

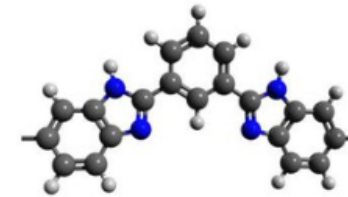
Extra no. 1

PBI membranes for HT-PEMFCs

HT-PEFCs run at an operating temperature of about 160 °C with membrane electrode assemblies (MEAs), based on a polybenzimidazole-type polymer loaded with phosphoric acid (H_3PO_4) – e.g. *m*-PBI or *ab*-PBI (see Fig. 1). In the temperature range between 160 °C and 180 °C, the polymers loaded with H_3PO_4 display very high proton conductivity, relatively low gas permeability, and good mechanical stability.

The high operating temperature above 100 °C has several advantages over low-temperature polymer membrane fuel cells (LT-PEMFCs), which are limited to operating temperatures below 80 °C.

m-PBI, Poly[2,2'-(*m*-phenylen)- 5,5' bibenzimidazol]



ab-PBI, Poly[2,5-benzimidazol]



Fig. 1: Repeating units of two polybenzimidazole-type polymers

<https://www.fz-juelich.de/en/iek/iek-14/research/pcl/spectroscopy/pbi-membranes>

Extra no. 2

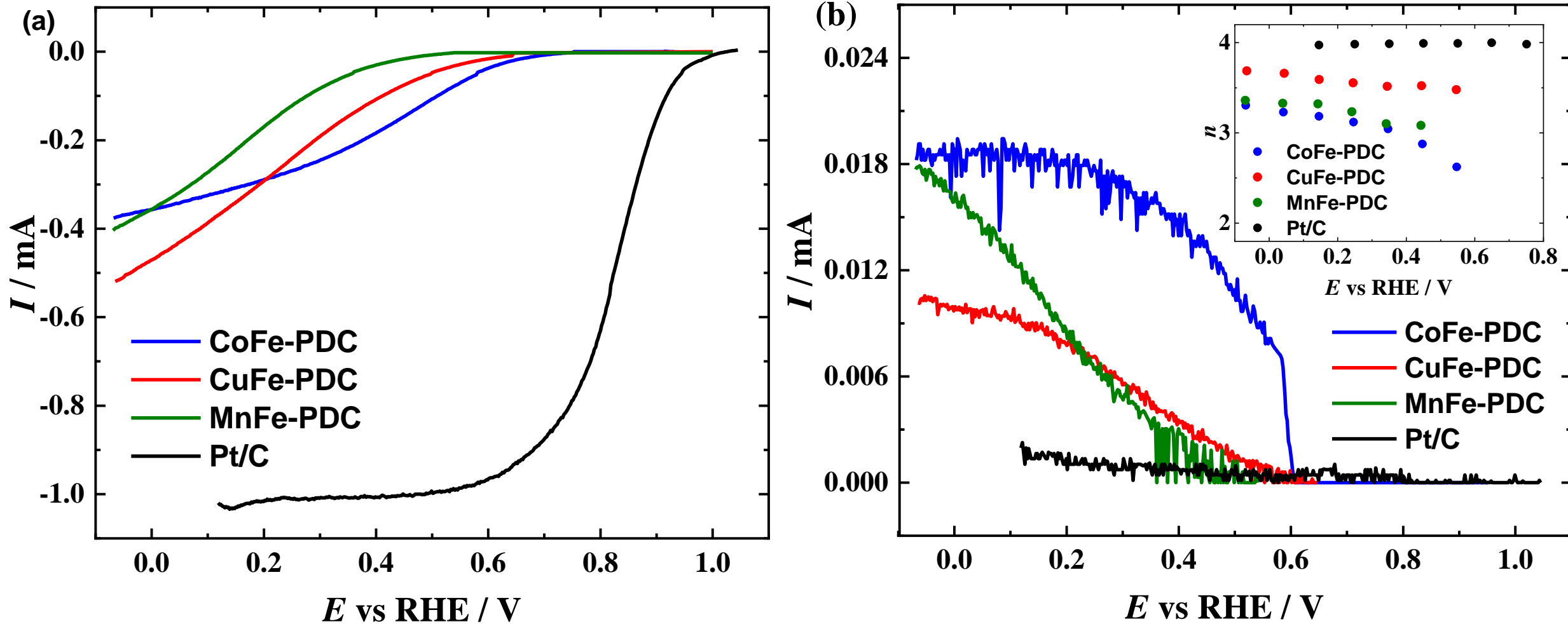


Fig. E1. (a) Disc current, (b) ring current and electron transfer numbers (n) for different catalyst coated GC-disk/Pt-ring electrodes recorded at 1600 rpm in O₂-saturated 0.5 M phosphoric acid solution.

Extra no. 3

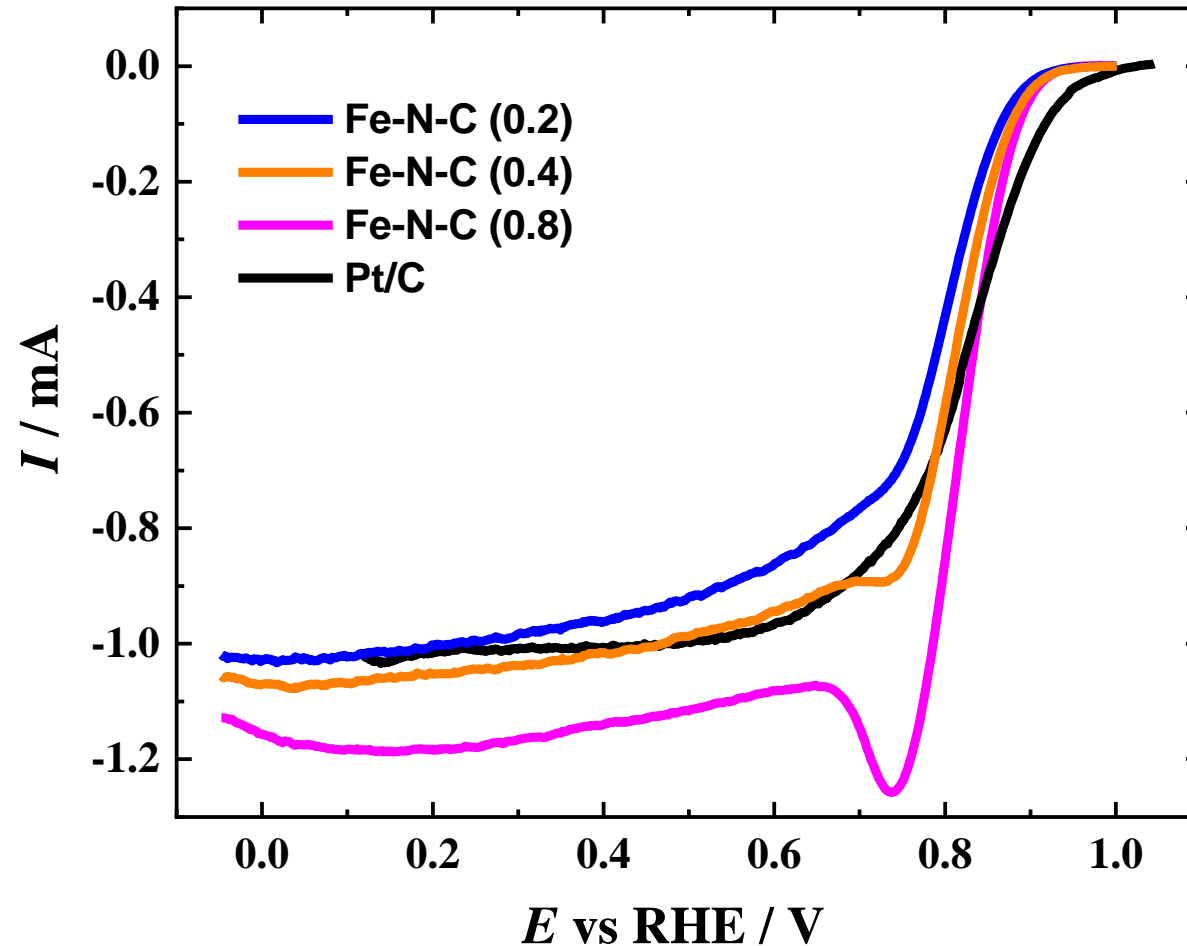


Fig. E2. RDE voltammetry curves for ORR recorded at 1600 rpm in O₂-saturated 0.5 M phosphoric acid solution with different loadings of commercial Fe-N-C catalyst (mg cm⁻²) and Pt/C (20 μg_{Pt} cm⁻²). Catalyst loading of 0.4 mg cm⁻² (PMF-0011904, Pajarito Powder) was chosen for comparison in this work.